Ionothermal Synthesis

DOI: 10.1002/ange.201102738

Ionothermal Synthesis and Structure Analysis of an Open-Framework Zirconium Phosphate with a High CO_2/CH_4 Adsorption Ratio**

Lei Liu, Jiangfeng Yang, Jinping Li, Jinxiang Dong, Dubravka Šišak, Marisa Luzzatto, and Lynne B. McCusker**

Zirconium phosphate materials have been investigated extensively because of their potential for application in the fields of ion-exchange, catalysis, photochemistry, and biotechnology.[1] Most studies of these materials have focused on the two layer compounds α-$Zr(HPO_4)_2{\cdot}H_2O$ and γ-$ZrPO_4(H_2PO_4){\cdot}2H_2O$ and their derivatives, which are obtained by post-synthesis processing techniques (for example ion-exchange, intercalation, or grafting).[2] The main reason most other zirconium phosphate materials have been neglected can probably be attributed to their poor thermostability. They have generally been synthesized using organic amines as structure-directing agents in a hydro-/solvothermal procedure.[2d,3] Of these templated zirconium phosphate materials, those with framework (rather than layer) structures tend to have a higher thermostability, but they are difficult to synthesize using this conventional synthetic approach. In fact, only two open-framework structures have resulted from these efforts.[4] Unfortunately, neither is stable to the removal of the occluded organic species by calcination, so they cannot be used as microporous materials for gas adsorption or separation, or for shape-selective catalysis.

Ionothermal syntheses, using ionic liquids or eutectic mixtures to serve as both the solvent and the structure directing agent, have some interesting features and advantages over the conventional approach to preparing crystalline porous materials.[5] Not only is the vapor pressure vanishingly small during the reaction process, but the chemistry of an ionic liquid is also quite different from that of a molecular solvent. This combination opens up new vistas for the synthesis of novel porous solids.[6] For example, ionothermal synthesis produced the first aluminophosphate molecular sieve with 20-ring pore openings (DNL-1, **-CLO** framework type).[6d] Recently, our group reported the ionothermal synthesis of a zirconium phosphate using a deep-eutectic solvent (DES), which consisted of carboxylic acid and quaternary ammonium salts. The resulting framework structure was found to depend on the structure and steric effect of the quaternary ammonium cation.[7]

Primary, secondary, and tertiary organic amines are easily protonated with hydrochloric acid to form organic ammonium chlorides, which can also be used to form DES with carboxylic acids or amides.[8] Such DES are easily prepared from readily available components and the diversity of their structures can be exploited to synthesize new porous solids using this emerging ionothermal procedure.

Herein, we combined ethylammonium chloride and oxalic acid to form a DES with a melting point below 100 °C, and then used it to synthesize a novel open-framework zirconium phosphate, $[(C_2H_7NH)_8(H_2O)_8][Zr_{32}P_{48}O_{176}F_8(OH)_{16}]$ (denoted hereafter as ZrPOF-EA). SEM images show that the crystallites have a flat needlelike morphology with dimensions of about $10\times2\times0.2\ \mu m^3$ (Supporting Information, Figure S1).

The crystal structure of ZrPOF-EA was solved from high-resolution powder diffraction data collected on the Swiss–Norwegian Beamline at the ESRF in Grenoble, France (Supporting Information, Table S1). The pattern was indexed in the orthorhombic system ($a=6.165$, $b=19.955$, $c=37.062$ Å) and reflection intensities were extracted assuming the space group $Pmc2_1$. These data were used as input to the powder charge-flipping (pCF) algorithm[9] in the program Superflip[10] for structure solution. The best electron density map from the first pCF run was used as a seed to generate the starting phase sets for the second run, and the best of the resulting maps was interpreted to yield the positions of all 16 zirconium, 23 of the 24 phosphorus, and 55 of the 77 oxygen atoms. Rietveld refinement, using the program XRS-82,[11] was initiated using this model, with the missing bridging oxygen atoms inserted. A series of difference electron density maps led to the location of the missing phsoporus atom, the terminal oxygen atoms, and the nonframework species. Atoms bridging between two zirconium atoms were assigned as fluorine.

During the course of the refinement, it became apparent that most of the framework atoms followed the symmetry of the higher space group *Pbam*, so refinement was completed in that space group even though it meant that the terminal P–

[*] Dr. L. Liu, J. F. Yang, Prof. J. P. Li, Prof. J. X. Dong
Research Institute of Special Chemicals
Taiyuan University of Technology
Taiyuan 030024, Shanxi (P.R. China)
E-mail: dongjinxiangwork@hotmail.com
D. Šišak, M. Luzzatto, Dr. L. B. McCusker
Laboratorium für Kristallographie, ETH Zürich
8093 Zürich (Switzerland)
E-mail: mccusker@mat.ethz.ch

[**] We thank the beamline scientists on the Swiss–Norwegian Beamline at the ESRF in Grenoble, France for their assistance with the powder diffraction measurements, and also thank Dr. Bo Xiao at Taiyuan University of Technology for helpful discussions on gas sorption analysis. The Chinese group was financially supported by the National Natural Science Foundation (Grant No. 20825623, 20801039) and the Program for the Top Science and Technology Innovation Teams and Top Young Academic Leaders of Higher Learning Institutions of Shanxi. The Swiss group gratefully acknowledges support from the Swiss National Science Foundation.

Supporting information for this article is available on the WWW under http://dx.doi.org/10.1002/anie.201102738.

OH groups and the organic cations were disordered. This refinement, with 8 zirconium, 12 phosphorus, 40 oxygen, 2 fluorine, 2 water, and 3 ethyl ammonium ions in the asymmetric unit, converged with the R values $R_F = 0.038$, and $R_{wp} = 0.170$ ($R_{exp} = 0.171$). Attempts to refine the structure in different subgroups of *Pbam* with different ordering of the P–OH groups were unsuccessful. It appears that both orientations of these phosphate tetrahedra are present. This phenomenon has also been observed in other zirconium phosphate framework materials.[4d,e] The final framework structure is shown in Figure 1. Further details regarding the structure analysis, including the location of the nonframework species (Figure S2), the dimensions of the pores (Figure S3), and the profile fit (Figure S4) are given in the supporting information.

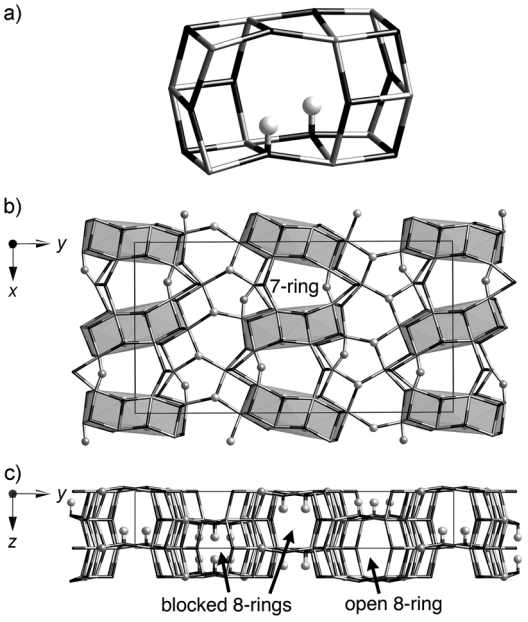

Figure 1. ZrPOF-EA framework structure showing a) the characteristic $[4^{14}8^2]$ unit, b) the projection along the *c* axis with the $[4^{14}8^2]$ units highlighted, and c) the projection along the *a* axis. Bridging O atoms have been omitted for clarity. Terminal O atoms and bridging F atoms are shown as balls, Zr gray, and P black.

The structure of ZrPOF-EA is complicated: it consists of $[4^{14}8^2]$ units arranged in a rectangular array connected by ZrO_6, ZrO_5F, and PO_4 linkages (Figure 1). There are 3-, 4-, 5-, 6-, 7-, and 8-ring units in the structure, and these form small one-dimensional channels parallel to the *c* (7-ring) and *a* (8-ring) axes. Open framework structures with 7- and 8-ring channels appear to be relatively rare, but some have been reported.[12]

Because some of the phosphorus atoms in ZrPOF-EA are only three-connected, there are terminal hydroxy groups, and as can be seen in Figure 1a and c, these block the 8-ring channels that would otherwise intersect the 7-ring channels to form a two-dimensional channel system. Furthermore, at least half of the remaining 8-ring channels, which do not intersect the 7-ring channels, are similarly blocked. In the as-synthesized form, ethylammonium cations and water molecules are occluded in the open channels and in the $[4^{14}8^2]$ units, respectively. In Figure 1c, the orientations of the terminal P–OH groups have been rationalized to avoid short contacts with the ethylammonium cations in the open channels (Supporting Information, Figure S2), but the arrangement can change from cell to cell, so some of these open 8-ring channels may also be blocked.

TGA and X-ray powder diffraction studies (Supporting Information, Figure S5, S6) show that the guest molecules occupying the channels of ZrPOF-EA can be removed by heating the material in air at 410 °C for 9 h without causing collapse of the host framework. To verify that the resulting porosity was indeed permanent, gas adsorption experiments were performed. The N_2 uptake at liquid nitrogen temperature was found to be extremely low (7.5 mL g^{-1} at 1 atm), indicating that the N_2 molecule had difficulty in accessing the channels, so CO_2 adsorption experiments were performed at 0 °C (Supporting Information, Figure S7). The surface area of ZrPOF-EA was calculated to be 166 $m^2 g^{-1}$ using the Dubinin–Radushkevitch (D-R) equation.[13] This relatively low surface area, which is slightly less than that of a typical microporous 8-ring zeolite, is consistent with the low number of guest molecules in the as-synthesized sample (only 4.4 wt% for ethylamine and 1.8 wt% for water) and its complicated pore structure with P–OH groups blocking some of the channels.

The separation of CO_2 from CH_4 is an important and difficult issue in the processing of low-quality natural gas, such as biogas or landfill gases. CO_2 impurities must be separated because the presence of CO_2 reduces the energy content of the natural gas and also causes corrosion of the storage tanks and pipelines owing to its acidity in a wet mixture.[14] Numerous 8-ring crystalline porous materials have been examined as candidates for the CO_2/CH_4 separation process,[15] because the effective pore width of a typical 8-ring (ca. 3.8 Å) is similar in size to the kinetic diameter of CH_4 (3.8 Å) but larger than that of CO_2 (3.3 Å). Those small-pore materials are usually prepared as membranes on α-Al_2O_3 supports for CO_2/CH_4 separation. The higher the CO_2/CH_4 adsorption ratio, the higher the CO_2/CH_4 separation selectivity of the membranes.[15b] Although a high CO_2/CH_4 adsorption ratio (ca. 29) was reported for SAPO-34 with small crystallites (0.5 μm),[16] in most cases the CO_2/CH_4 adsorption ratio is quite low (around 6.0) for these polycrystalline materials (for example, SAPO-34, SAPO-43, AlPO-14, and all-silica zeolite deca-dodecasil 3R).[17] CH_4 molecules can still penetrate the 8-ring windows. It stands to reason that materials with pore openings smaller than the kinetic diameter of CH_4 but larger than that of CO_2 would be particularly well-suited to improving the CO_2/CH_4 adsorption capacity ratio.

In ZrPOF-EA, the oval 7- and 8-ring windows have dimensions of about 4.0 × 3.0 Å and 3.9 × 3.2 Å, respectively (Supporting Information, Figure S3). To establish its adsorption properties, CO_2, N_2, and CH_4 adsorption experiments were carried out on an intelligent gravimetric analyzer (IGA-001, Hiden Isochema) at 25 °C. Before each adsorption experiment, the activated ZrPOF-EA was outgassed at 300 °C under vacuum for 10 h. From the adsorption isotherms

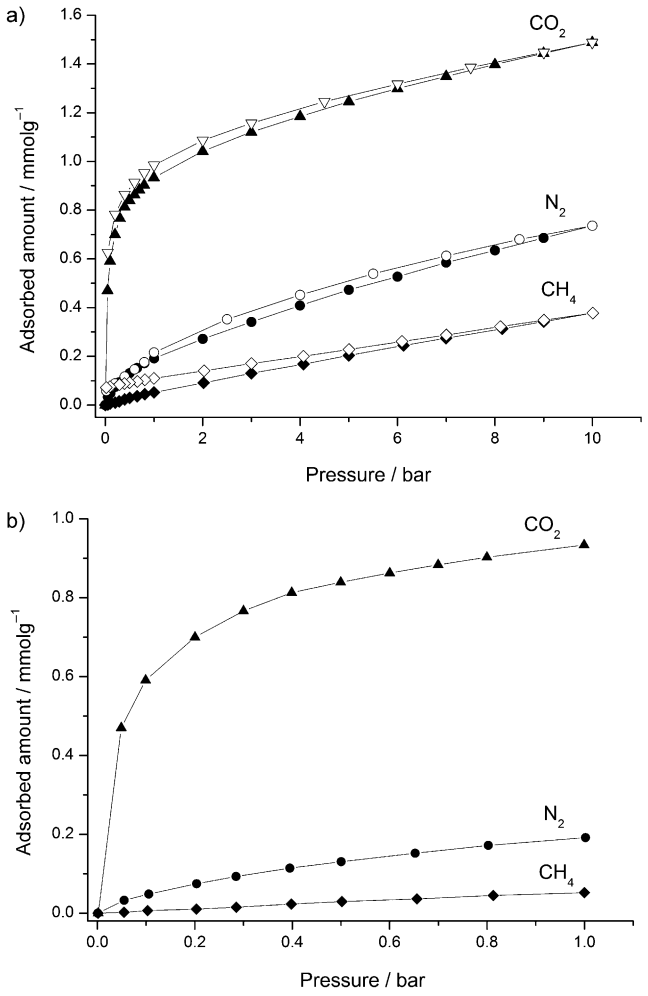

Figure 2. a) Adsorption and desorption isotherms of CO_2, N_2, and CH_4 for ZrPOF-EA at 25 °C, and b) expanded view of the low-pressure range (0–1 bar). Filled symbols: adsorption, open symbols: desorption.

shown in Figure 2, it is evident that the adsorption capacity for CO_2 is markedly higher than that for CH_4, with a CO_2/CH_4 adsorption ratio ranging from 67.2 at 0.2 bar to 17.3 at 1 bar. The selective adsorption of CO_2 may be a result of the complicated pore structure and the polar hydroxy groups directed into the pore channels.[18] The small 7- and 8-ring pore openings allow CO_2 molecules (3.3 Å kinetic diameter) to enter the channels, but block the larger CH_4 molecules (3.8 Å kinetic diameter). Furthermore, the low N_2 adsorption capacity indicates that even the intermediate-sized N_2 (3.6 Å kinetic diameter) has difficulty in entering the pores, leading to a CO_2/N_2 adsorption ratio ranging from 12.2 at 0.2 bar to 4.9 at 1 bar. The N_2 adsorption capacity at 1 bar (0.19 mmol g^{-1}) is slightly higher than that of CH_4 (0.05 mmol g^{-1}), because N_2 has a slightly smaller kinetic diameter than CH_4, so it is easier for N_2 to enter the channels. At high pressures, however, the CO_2 selectivity decreases (3.9 for CO_2/CH_4 and 2.0 for CO_2/N_2 at 10 bar), because the framework is flexible[19] and the gas diffusion velocity increases. More of the larger CH_4 or N_2 molecules can squeeze through the small pore openings, while the smaller CO_2 molecules have been already approached saturation state at low pressure.

The desorption isotherms of CO_2 and CH_4 are slightly higher than the adsorption isotherms, indicating that the adsorption is nearly reversible. A second cycle of ad- and desorption isotherms (Supporting Information, Figure S8) after treating ZrPOF-EA at 50 °C under vacuum for 6 h shows that the readsorption capacity for CO_2 and CH_4 is comparable to the initial adsorption capacity and the CO_2/CH_4 adsorption ratio is 17.5 at 1 bar. ZrPOF-EA has a notably higher CO_2/CH_4 adsorption ratio (ca. 17 at 1 bar) than for example SAPO-43 (6.68 at 1 bar), a typical 8-ring molecular sieve with 4.5×3.1 Å pore openings.[17f] It seems that ZrPOF-EA, with its small 7- and 8-ring channels, is a highly effective size-selective molecular sieve that can discriminate between CO_2 and CH_4 at room temperature.

One of the applications of CO_2 separation technologies is in the upgrade of biogas to pure or more concentrated methane. Biogas, which is essentially a mixture of CO_2 (ca. 25–45 %) and CH_4, is a very important source of renewable methane produced by the anaerobic digestion of waste materials.[20] Although ZrPOF-EA has a relatively low adsorption capacity, its high CO_2/CH_4 adsorption ratio may find industrial application in membrane separation technology for upgrading such natural gas.

In conclusion, from a deep-eutectic solvent composed of oxalic acid and ethylammonium chloride, we synthesized a novel open-framework zirconium phosphate with small 7- and 8-ring channels. Water and organic species could be removed by calcination to produce a material with permanent porosity. This porous material shows a remarkable CO_2/CH_4 adsorption ratio that is significantly higher than that exhibited by conventional 8-ring pore materials. ZrPOF-EA is a highly effective size-selective molecular sieve that can discriminate between CO_2 and CH_4, making it attractive for processes requiring CO_2/CH_4 separation.

Experimental Section

Typical synthesis of ZrPOF-EA: a Teflon-lined autoclave (total volume 23 mL) was charged with DES made from oxalic acid dihydrate (2.0 g, 15.88 mmol) and ethylammonium chloride (2.0 g, 24.50 mmol), $ZrOCl_2 \cdot 8H_2O$ (250 mg, 0.76 mmol), H_3PO_4(177 mg, 1.54 mmol), and HF (75 μL, 1.73 mmol). The autoclave was then heated at 180 °C for 4 days and then cooled to room temperature. The solid product was washed thoroughly with acetone and water, and dried at room temperature. Elemental analysis (%) calcd for ZrPOF-EA: C 2.36, H 1.18, N 1.37, Zr 35.72; P 18.25, F 1.87; found: C 2.49, H 1.25, N 1.42, Zr 36.18, P 18.10, F 1.90. The experimental characterization techniques, including SEM images, TGA curves, calculated and observed X-ray powder diffraction patterns, gas adsorption isotherm, and crystallographic data are described in detail in the Supporting Information. Further details of the crystal structure investigation may be obtained from the Fachinformationszentrum Karlsruhe, 76344 Eggenstein-Leopoldshafen, Germany (fax: (+49) 7247-808-666; e-mail: crysdata@fiz-karlsruhe.de), on quoting the depository number CSD-422959 (ZrPOF-EA).

Caution: HF (48 wt% in water) is very toxic when inhaled, in contact with skin, or swallowed. When used, suitable protective clothing (gloves and eye/face protection) must be worn.

Received: April 20, 2011
Revised: May 31, 2011
Published online: July 7, 2011

Keywords: gas adsorption · ionothermal synthesis · open frameworks · separation · zirconium phosphates

[1] a) G. Alberti, M. Casciola, U. Costantino, R. Vivani, *Adv. Mater.* **1996**, *8*, 291 – 303; b) G. Cao, M. E. Garcia, M. Alcalá, L. F. Burges, T. E. Mallouk, *J. Am. Chem. Soc.* **1992**, *114*, 7574 – 7575; c) M. B. Santiago, C. Declet-Flores, A. Diaz, M. M. Velez, M. Z. Bosques, Y. Sanakis, J. L. Colon, *Langmuir* **2007**, *23*, 7810 – 7817; d) C. V. Kumar, A. Chaudhari, *J. Am. Chem. Soc.* **2000**, *122*, 830 – 837.

[2] a) G. Alberti, S. Murcia-Mascarós, R. Vivani, *J. Am. Chem. Soc.* **1998**, *120*, 9291 – 9295; b) E. Brunet, H. M. H. Alhendawi, C. Cerro, M. J. de La Mata, O. Juanes, J. C. Rodríguez-Ubis, *Angew. Chem.* **2006**, *118*, 7072 – 7074; *Angew. Chem. Int. Ed.* **2006**, *45*, 6918 – 6920; c) T. Takei, Y. Kobayashi, H. Hata, Y. Yonesaki, N. Kumada, N. Kinomura, T. E. Mallouk, *J. Am. Chem. Soc.* **2006**, *128*, 16634 – 16640; d) R. Vivani, G. Alberti, F. Costantino, M. Nocchetti, *Microporous Mesoporous Mater.* **2008**, *107*, 58 – 70.

[3] R. Murugavel, A. Choudhury, M. G. Walawalkar, R. Pothiraja, C. N. R. Rao, *Chem. Rev.* **2008**, *108*, 3549 – 3655.

[4] a) E. Kemnitz, M. Wloka, S. Trojanov, A. Stiewe, *Angew. Chem.* **1996**, *108*, 2809 – 2811; *Angew. Chem. Int. Ed.* **1996**, *35*, 2677 – 2678; b) M. Wloka, S. I. Trojanov, E. Kemnitz, *J. Solid State Chem.* **1998**, *135*, 293 – 301; c) M. Wloka, S. I. Trojanov, E. Kemnitz, *Z. Anorg. Allg. Chem.* **1999**, *625*, 1028 – 1032; d) M. Wloka, S. I. Trojanov, E. Kemnitz, *J. Solid State Chem.* **2000**, *149*, 21 – 27; e) J. X. Dong, L. Liu, J. P. Li, Y. Li, Ch. Baerlocher, L. B. McCusker, *Microporous Mesoporous Mater.* **2007**, *104*, 185 – 191.

[5] a) E. R. Cooper, C. D. Andrews, P. S. Wheatley, P. B. Webb, P. Wormald, R. E. Morris, *Nature* **2004**, *430*, 1012 – 1016; b) E. R. Parnham, R. E. Morris, *Acc. Chem. Res.* **2007**, *40*, 1005 – 1013; c) R. E. Morris, *Chem. Commun.* **2009**, 2990 – 2998; d) E. R. Parnham, R. E. Morris, *J. Am. Chem. Soc.* **2006**, *128*, 2204 – 2205.

[6] a) H. Xing, J. Li, W. Yan, P. Chen, Z. Jin, J. Yu, S. Dai, R. Xu, *Chem. Mater.* **2008**, *20*, 4179 – 4181; b) L. Liu, S. Ferdov, C. Coelho, K. Kong, L. Mafra, J. P. Li, J. X. Dong, U. Kolitsch, R. S. Ferreira, E. Tillmanns, J. Rocha, Z. Lin, *Inorg. Chem.* **2009**, *48*, 4598 – 4600; c) H. Xing, W. Yang, T. Su, Y. Li, J. Xu, T. Nakano, J. Yu, R. Xu, *Angew. Chem.* **2010**, *122*, 2378 – 2381; *Angew. Chem. Int. Ed.* **2010**, *49*, 2328 – 2331; d) Y. Wei, Z. Tian, H. Gies, R. Xu, H. Ma, R. Pei, W. Zhang, Y. Xu, L. Wang, K. Li, B. Wang, G. Wen, L. Lin, *Angew. Chem.* **2010**, *122*, 5495 – 5498; *Angew. Chem. Int. Ed.* **2010**, *49*, 5367 – 5370.

[7] a) L. Liu, Y. Li, H. B. Wei, M. Dong, J. G. Wang, A. M. Z. Slawin, J. P. Li, J. X. Dong, R. E. Morris, *Angew. Chem.* **2009**, *121*, 2240 – 2243; *Angew. Chem. Int. Ed.* **2009**, *48*, 2206 – 2209; b) L. Liu, Z. F. Chen, H. B. Wei, Y. Li, Y. C. Fu, H. Xu, J. P. Li, A. M. Z. Slawin, J. X. Dong, *Inorg. Chem.* **2010**, *49*, 8270 – 8275.

[8] A. P. Abbott, G. Capper, S. Gray, *ChemPhysChem* **2006**, *7*, 803 – 806.

[9] a) G. Oszlányi, A. Sütő, *Acta Crystallogr. Sect. A* **2004**, *60*, 134 – 141; b) Ch. Baerlocher, L. B. McCusker, L. Palatinus, *Z. Kristallogr.* **2007**, *222*, 47 – 53.

[10] L. Palatinus, G. Chapuis, *J. Appl. Crystallogr.* **2007**, *40*, 786 – 790.

[11] Ch. Baerlocher, *The X-ray Rietveld System (XRS-82)*, Laboratory of Crystallography, ETH Zurich, **1982**.

[12] a) J. J. Lu, Y. Xu, N. K. Goh, L. S. Chia, *Chem. Commun.* **1998**, 1709 – 1710; b) A. Matijasic, V. Gramlich, J. Patarin, *J. Mater. Chem.* **2001**, *11*, 2553 – 2559.

[13] N. D. Hutson, R. T. Yang, *Adsorption* **1997**, *3*, 189 – 195.

[14] a) H. Lin, E. Van Wagner, R. Raharjo, B. D. Freeman, I. Roman, *Adv. Mater.* **2006**, *18*, 39 – 44; b) M. A. Carreon, S. Li, J. L. Falconer, R. D. Noble, *J. Am. Chem. Soc.* **2008**, *130*, 5412 – 5413.

[15] a) S. Li, J. G. Martinek, J. L. Falconer, R. D. Noble, *Ind. Eng. Chem. Res.* **2005**, *44*, 3220 – 3228; b) M. A. Carreon, S. Li, J. L. Falconer, R. D. Noble, *Adv. Mater.* **2008**, *20*, 729 – 732.

[16] S. R. Venna, M. A. Carreon, *J. Mater. Chem.* **2009**, *19*, 3138 – 3140.

[17] a) S. Himeno, T. Tomita, K. Suzuki, K. Nakayama, K. Yajima, S. Yoshida, *Ind. Eng. Chem. Res.* **2007**, *46*, 6989 – 6997; b) T. Tomita, K. Nakayama, H. Sakai, *Microporous Mesoporous Mater.* **2004**, *68*, 71 – 75; c) S. Siamak Ashraf Talesh, S. Fatemi, S. J. Hashemi, M. Ghasemi, *Sep. Sci. Technol.* **2010**, *45*, 1295 – 1301; d) X. X. Zhao, X. L. Xu, L. L. Sun, X. Q. Liu, *Energy Fuels* **2009**, *23*, 1534 – 1538; e) S. Himeno, T. Tomita, K. Suzuki, S. Yoshida, *Microporous Mesoporous Mater.* **2007**, *98*, 62 – 69; f) A. J. Hernández-Maldonado, R. T. Yang, D. Chinn, C. L. Munson, *Langmuir* **2003**, *19*, 2193 – 2200; g) S. R. Venna, M. A. Carreon, *Langmuir* **2011**, *27*, 2888 – 2894; h) S. R. Venna, M. A. Carreon, *J. Phys. Chem. B* **2008**, *112*, 16261 – 16265; i) S. Li, J. L. Falconer, R. D. Noble, *Microporous Mesoporous Mater.* **2008**, *110*, 310 – 317.

[18] M. Mastalerz, M. W. Schneider, I. M. Oppel, O. Presly, *Angew. Chem.* **2011**, *123*, 1078 – 1083; *Angew. Chem. Int. Ed.* **2011**, *50*, 1046 – 1051.

[19] a) R. Krishna, J. M. Van Baten, *Microporous Mesoporous Mater.* **2011**, *137*, 83 – 91; b) A. García-Sánchez, D. Dubbeldam, S. Calero, *J. Phys. Chem. C* **2010**, *114*, 15068 – 15074.

[20] J. Xuan, M. Leung, D. Leung, M. Ni, *Renewable Sustainable Energy Rev.* **2009**, *13*, 1301 – 1313.

